symmetry

MDPI

Article

Decay Law of Supercritical CO_2 Phase Transition-Induced Shock Waves in Rocky Media

Jie Zhang [1,2], Qifu Zeng [3,*], Fangqiang Wei [1,2], Lu Liu [3], Fayou Wu [3] and Haotian Li [3]

[1] College of Engineering, Tibet University, Lhasa 850000, China; 15826192123@163.com (J.Z.); fqwei@imde.ac.cn (F.W.)
[2] Chongqing Institution of Green and Intelligent Technology, Chinese Academy of Sciences, Chongqing 400714, China
[3] Chongqing Municipal Key Laboratory of Geological Disaster Reduction of Mountain Highway and Water Transport, Chongqing Jiaotong University, Chongqing 400074, China; m18723358016_1@163.com (L.L.); wfyou2020@126.com (F.W.); 622210960044@mails.cqjtu.edu.cn (H.L.)
* Correspondence: zengqifu2513@126.com

Abstract: Supercritical CO_2 phase change fracturing technology has been widely used in rock engineering, with the advantages of low disturbance and no pollution. However, the phase change shock wave inevitably affects the surrounding environment, and the influence range is still unclear. In this paper, we present a computational model for the symmetric generation, propagation, and attenuation of supercritical CO_2 phase transition shock waves, with the center of the borehole as the origin, based on the C–J theory. The attenuation of the shock wave in the rock medium under the influence of the type of fracturing tube, the thickness of the shear sheet, and the rock performance parameters are further analyzed. The results show that the rock stress under the action of the phase change shock wave attenuates logarithmically with the propagation distance, which correlates with the magnitude of the incident rock stress at the borehole wall. The incident rock stress decreases with the increase in the initial density of CO_2 in the fracturing tube, increases linearly with the thickness of the shear sheet, and correlates with the rock wave impedance.

Keywords: supercritical CO_2; shock wave; borehole wall incident rock stress; attenuation equation

check for updates

Citation: Zhang, J.; Zeng, Q.; Wei, F.; Liu, L.; Wu, F.; Li, H. Decay Law of Supercritical CO_2 Phase Transition-Induced Shock Waves in Rocky Media. *Symmetry* **2023**, *15*, 1802. https://doi.org/10.3390/sym15091802

Academic Editors: Mingdong Wei, Weigang Shen, Hongbo Du and Peng Feng

Received: 16 August 2023
Revised: 11 September 2023
Accepted: 20 September 2023
Published: 21 September 2023

Copyright: © 2023 by the authors. Licensee MDPI, Basel, Switzerland. This article is an open access article distributed under the terms and conditions of the Creative Commons Attribution (CC BY) license (https://creativecommons.org/licenses/by/4.0/).

1. Introduction

Traditional explosive rock breaking technology has been gradually regulated or even banned due to its high risk and high pollution [1]. As an alternative rock breaking technology, supercritical CO_2 phase change rock breaking has received more and more attention in the field of rock breaking due to its advantages of no sparks in the fracturing process and no pollution of the phase change products [2,3]. The technology was originated by the United Kingdom Cardox company, who developed a physical blasting device, mainly consisting of an inflatable head, heat pipe, liquid storage tube, sealing ring, shear blade energy release head, and six other major components, which are the main working media of liquid CO_2 blasting equipment [4,5]. The principle is to heat the heating tube so that the liquid CO_2 inside the fracturing tube rapidly realizes the phase change, and thus the volume of the instantaneous expansion of a strong pressure to achieve effective rock breaking, which conforms to the green and environmentally friendly method of rock breaking [6,7]. The technology was introduced to China by Guo Zhixing and Xu Ying, and has been gradually applied to the various fields of engineering and construction [8,9]. However, the blasting process is complex and short, the shock waves generated during rock breaking will inevitably affect the neighboring buildings and the surrounding environment [10], and the powerful shock disturbance can easily damage the neighboring building's, structures, and even risk the safety of civilians [11]. Therefore, an in-depth understanding of the

propagation and attenuation of supercritical CO_2 phase change shock waves in the rock mass is essential.

Existing views are generally that the supercritical CO_2 phase change rock breaking project concerning rock fragmentation is essentially the result of a shock wave and high-energy gases working together [12]. In the CO_2 phase change blasting process, a shear blade rupture CO_2 high-pressure gas shock wave is formed, and the initial peak shock pressure size and CO_2 charge and shear blade thickness are highly correlated, of which the thickness of the shear blade is the main control variable [13,14]. After the high-pressure gas impacts the rock body, incident rock body stress is formed, which is greater than the rock body rupture pressure, and the rock body becomes damaged. Regarding the rupture pressure of CO_2 phase change-impacted rock mass, the most widely used method is the TNT equivalent method, which considers the fact that the rupture pressure is related to the volume of the CO_2 reservoir tube, the strength of the shear sheet, and the external pressure of the fracturing tube [15]. In addition, Sun [16] fitted the corresponding working conditions using Matlab, and combined the rock breaking pressure magnitude with the JWL equation; alternatively, Guo [17] performed an energy analysis on the root-mean-square (RMS) of vibration data to quantify the total energy of the rock breakage. Taken together, there are fewer studies using stress wave theory to analyze the rupture pressure of CO_2 phase change-shocked rock. On the other hand, shock waves are characterized by short durations and fast decay rates, which are not easy to measure in practical engineering; thus, a large number of scholars have used the decay curves of the Plasma Point Vibration Velocity (PPV) to characterize the decay trend of the shock waves, based on which, they have carried out a large number of CO_2 phase change blasting on-site vibration tests. Among them, Renyou Ruan [18] found that PPV decayed exponentially with distance through the foundation vibration test of step excavation, whereas Baolin Li [19] believed that its decay is in the form of a power function, and the steeper the slope, the faster the PPV decay. Shengtao Zhou [20] found that the crack growth rate after CO_2 blasting also reduces spatial growth at any time. Shibing Cheng [21] found that PPV varied with the distance from the center of the blast as a logarithmic function during the excavation of the pit of a comprehensive pipeline corridor. It can be seen that the field test alone may not reveal the essential law of CO_2 phase change blasting shock wave attenuation in the rock mass.

In summary, it can be seen that, at present, the use of stress wave theory to study the supercritical CO_2 phase transition shock waves under the action of the rock body rupture pressure calculation model is relatively limited, and the shock wave attenuation law needs more in-depth theoretical analysis. For this reason, this paper, according to the hydrodynamic burst theory, combined with the supercritical CO_2 phase change-induced shock wave characteristics, presents the establishment of the supercritical CO_2 phase change process of pressure, density, and rate of dynamic change of the kinetic model. On this basis, we further analyzed the thickness of the shear sheet, the rock performance parameters of the impact of the borehole wall of the incident rock stress, and finally, we consider the diffusion of the geometric wavefront as well as the influence of their material damping. In addition, we present the rock stress and vibration velocity decay equations under the action of the phase change shock wave.

2. Analysis of Characterization Value of Supercritical CO_2 Shock Wave

2.1. Supercritical CO_2 Phase Change Blast Gas State Parameter Analysis

1. Supercritical CO_2 phase change blast shock wave generation principle

The principle of supercritical CO_2 phase change fracturing is shown in Figure 1. After the heat pipe is excited and exothermic, the supercritical CO_2 in the liquid storage pipe rapidly realizes the transition from the supercritical state to the gas state, which leads to a rapid expansion in CO_2 volume, and the pressure inside the fracturing pauperizes rapidly. Similar to previous studies [22], when the pressure inside the pipe exceeds the ultimate shear strength of the shear sheet, the shear sheet ruptures, and the high-pressure CO_2 gas

is sprayed out of the relief holes. The phase change impact load is applied to the rock body with the center of the borehole as the origin, acting symmetrically on the wall of the borehole, and further attenuating to the surrounding area to realize the task of impact rock breaking.

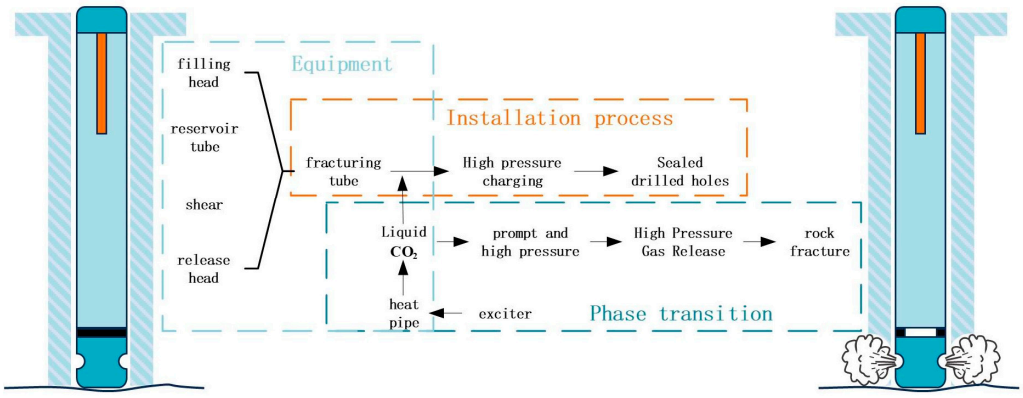


Figure 1. Schematic diagram of supercritical CO2 phase transition fracturing.

After the rupture of the shear sheet, the high-energy CO_2 gas rushes out rapidly, which generates a strong perturbation to the surrounding medium. Analogizing the perturbation process to the piston movement, the state parameters of the shock wave during the movement of the wavefront surface from the 1-1′ cross-section to the 2-2′ cross-section are shown in Figure 2. Under one-dimensional shock conditions, the CO_2 phase transition shock velocity is denoted by D. The CO_2 density, pressure, mass velocity, temperature, and specific thermodynamic energy in the initial state before the shock wave are denoted by ρ_0, p_0, u_0, T_0, and e_0, respectively, and the corresponding state parameters of the shock wave blast gas are denoted by ρ_H, p_0, u_H, T_H, and e_H, respectively.

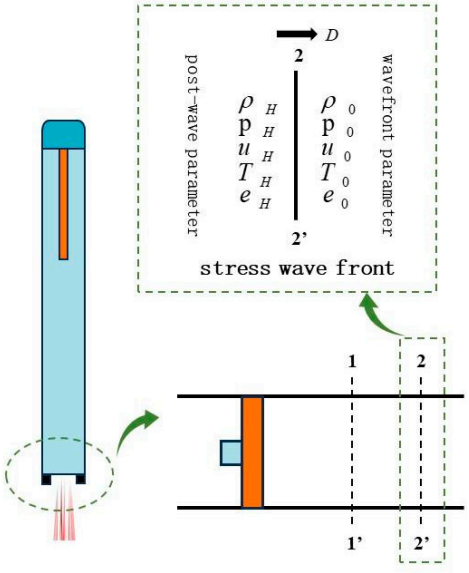


Figure 2. Schematic diagram of shock wave generation.

2. Derivation of shock wave state parameters for supercritical CO_2 phase change blasting

Unlike explosive blast waves, supercritical CO_2 phase change shock waves do not carry chemical reactions, but still follow the three conservation laws of mass, momentum, and energy. Assuming that the initial mass velocity is $u_0 = 0$ at the instant of shear sheet rupture, the following equation can be obtained according to the three conservation laws [23]:

Mass conservation relationship:

$$\rho_0 D = \rho_H (D - u_H) \tag{1}$$

Conservation of momentum relationship:

$$\rho_0 D u_H = p_H - p_0 \tag{2}$$

Energy conservation relationship:

$$\rho_0 D e_0 + \frac{1}{2}\rho_0 D^3 + p_0 D = \rho_H (D - u_H) e_H + \frac{1}{2}\rho_H (D - u_H)^3 + p_H (D - u_H) \tag{3}$$

The first term on the left side of the energy equation represents the internal energy of the substance, the second term represents the kinetic energy of the medium movement, and the third term represents the pressure potential energy. The right side of the equation represents the internal energy of the substance, the kinetic energy of the medium, and the pressure potential energy of the supercritical CO_2 phase change explosion, in that order.

Introducing the mass volume of the initial state before supercritical CO_2 phase change blasting $V_0 = 1/\rho_0$ and the mass volume of the blasting products $V_H = 1/\rho_H$, the shock wave velocity can be obtained by substituting the following into Equations (1) and (2):

$$D = V_0 \sqrt{(p_H - p_0)/(V_0 - V_H)} \tag{4}$$

Equations (2) and (4) give the product velocity u_H after shock wave perturbation as

$$u_H = \sqrt{(p_H - p_0)(V_0 - V_H)} \tag{5}$$

Considering the CO_2 gas before and after the wavefront surface as an ideal gas, the ideal gas equation of state can be obtained:

$$p_H V_H = R T_H / M_H \tag{6}$$

where R is the molar gas constant and M_H is the molar mass of the blast gas product.

Using the equation of state for an ideal gas, the internal energy of an ideal gas can be expressed as

$$e_H = \frac{p_H V_H}{k-1},\ e_0 = \frac{p_0 V_0}{k-1} \tag{7}$$

where k is the specific heat ratio of the blast product, generally taken as 1.29.

The steady propagation condition of the blast shock wave according to the C–J theory is obtained as follows:

$$D_H = C_H + u_H \tag{8}$$

where C_H is the speed of sound of the product on the blast wave front, m/s; D_H is the propagation speed of the blast wave, m/s.

Using Equation (9) and the equation of state for the isentropic expansion process ($pV^k = A$ constant) results in

$$\frac{p_H}{V_0 - V_H} = -\left.\frac{dp}{dV}\right|_S = \frac{k p_H}{V_H} \rightarrow V_H = \frac{k}{k+1} V_0 \tag{9}$$

It can be obtained from Equations (4) and (9) that

$$D = V_0 \sqrt{\frac{k p_H}{V_H}} \rightarrow \rho_0 D^2 = k p_H \frac{V_0}{V_H} = (k+1) p_H \rightarrow p_H = \frac{1}{k+1}\rho_0 D^2 \tag{10}$$

By substituting Equations (9) and (10) into the ideal gas equation of state (Equation (6)), the following is obtained:

$$T_H = \frac{M_H}{R} \frac{k}{(k+1)^2} D^2 \tag{11}$$

At this point, all the state parameters of the supercritical CO_2 phase change blast shock wave have been derived.

2.2. Supercritical CO_2 Phase Transition Shock Test

As mentioned before, supercritical CO_2 phase transition shock pressure and shock wave velocity are important parameters for shock wave characterization. If we want to obtain the shock wave velocity, we must obtain both the supercritical CO_2 phase transition shock pressure and the gas volume after the explosion. However, the phase transition shock pressure is not easy to obtain, so the supercritical CO_2 phase transition shock test is carried out to analyze the shock wave pressure law.

The test system is a supercritical CO_2 phase change pulse pressure test system designed by Chongqing Jiaotong University [24,25], and includes a CO_2 charging system, a phase change bursting system, and a data acquisition system, which can realize the functions of CO_2 charging and the pressure and temperature control during the charging process, the bursting control of fracturing tubes, and the data acquisition, etc. The physical diagram is shown in Figure 3. Compared with the Cardox device developed in the UK, this device incorporates a computerized control system, which is able to accurately control the quality, design pressure, and temperature of the CO_2 to be filled into the reservoir tube in liquid form. Compared with the original device, it is more precise and intelligent, safer, and more efficient.

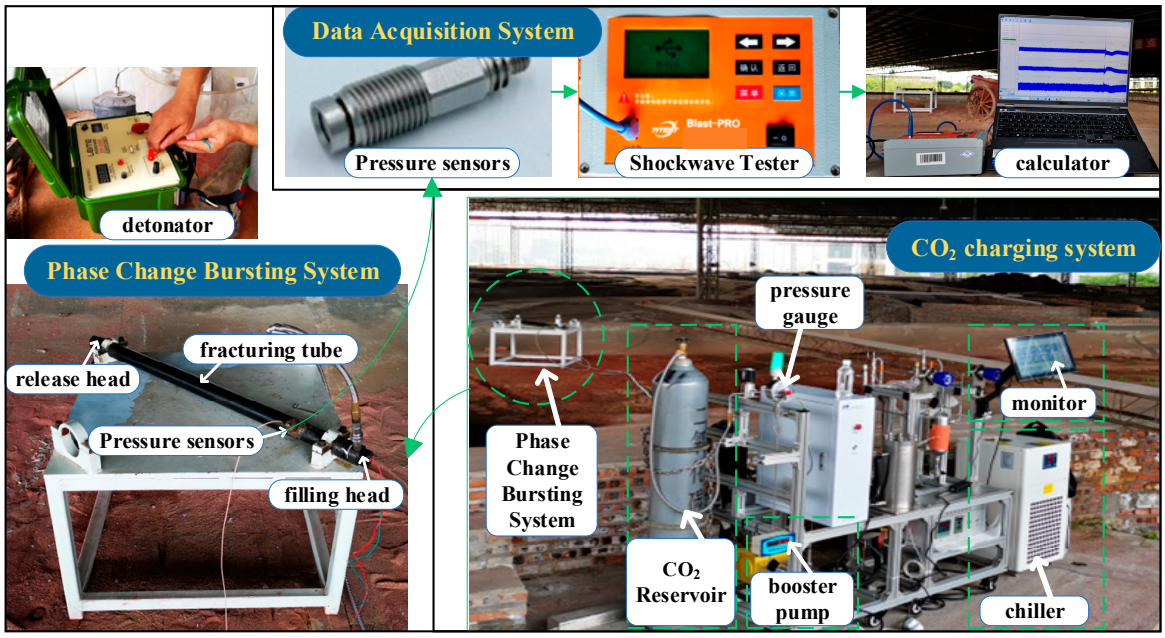


Figure 3. Physical diagram of supercritical CO_2 phase change impact test system.

The test was carried out using a 51-type fracturing tube with a length of 1 m, an inner diameter of 23 mm, a volume of 5.8×10^{-2} m, and a mass of 900 g of fillable CO_2. The shear plate used in the test was made of Q235 steel, with a shear strength of 165 MPa, and the radius of the releasing hole was 11 mm. Eight groups of tests were carried out according to the quality of the activator, the thickness of the shear plate, and in combination with the principle of an orthogonal test. The test conditions were shown in Table 1.

Table 1. Experimental design conditions.

Serial Number	Fracturing Tube Models	Activator Mass/g	Shear Thickness/mm
1	51	70	3.4
2	51	70	2.6
3	51	90	3.4
4	51	90	2.6
5	51	90	1.9
6	51	120	2.6
7	51	120	1.9
8	51	120	3.4

At the end of the test, the shear piece ruptured along the prongs of the safety valve body, and the shock wave pressure was characterized by a triangular pulse, i.e., a rapid rise before the peak and a sharp fall after the peak, as shown in Figure 4.

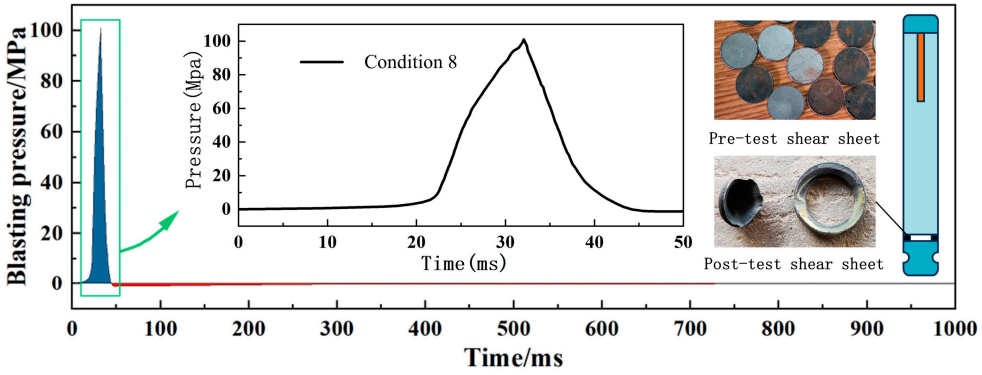


Figure 4. Typical test pressure curve.

Recent studies have shown that the shear sheet thickness is the main control variable for the impact pressure of supercritical CO_2 phase change bursting. To verify this conclusion, the experimental results are compared with the shear sheet damage equation in Figure 5.

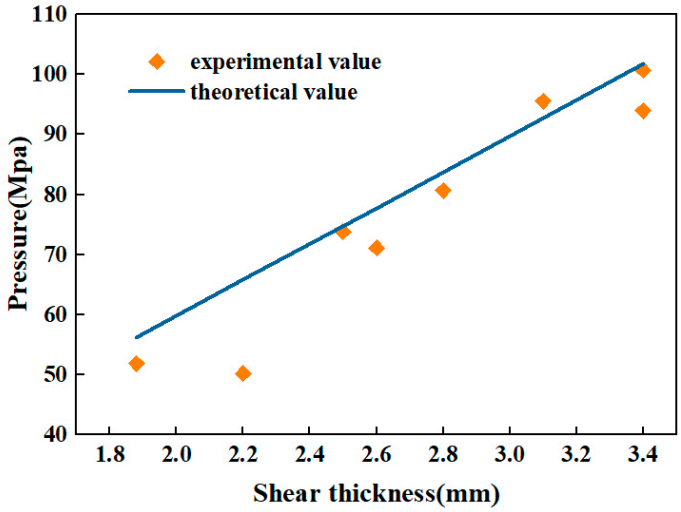


Figure 5. Comparison of peak pressure test value and calculated value.

As can be seen from Figure 5, the experimental results are similar to those of previous studies [13,14], and the shear damage equation fits the experimental test shock wave peak pressure well. Therefore, the shear damage formula can replace the supercritical CO_2 phase

transition shock pressure in Equation (10) for calculation. The shear damage equation is as follows:

$$P_H = \frac{2\sigma_s \delta}{R} \tag{12}$$

where P_H is the supercritical CO_2 blast pressure, MPa; R is the radius of the release hole, mm; σ_s is the material shear strength, MPa; δ is the thickness of the shear sheet, mm.

Substituting Equations (9) and (12) into Equation (10) yields (since $P_0 \ll P_H P_0$ is negligible) the following:

$$D = \left[\frac{2\sigma_s \delta(\mathrm{k}+1)}{R\rho_0}\right]^{1/2} \tag{13}$$

It can be seen that the shock wave velocity is mainly related to the thickness of the shear sheet and the initial density of CO_2 in the case of the same steel used for the fracturing tube and the same radius of the release hole.

3. Decay Law of Supercritical CO_2 Phase Change Shock Wave

3.1. Modeling the Propagation of Supercritical CO_2 Phase Change Shock Waves in Rocky Media

As shown in Figure 6, the supercritical CO_2 phase change shock wave loads the rock by impacting the pore wall after a short propagation period in the air, and the process is accompanied by the transmission and reflection of the shock wave at the pore wall. Assuming that the impact of the shock wave on the borehole wall is positive, the transmission and reflection parameters in the rock can be solved according to the positive incidence. The incident wave parameters are the same as the previous parameters; the transmission wave parameters are P_2, ρ_2, and u_2; the wave speed is D_2; and the initial parameters of the rock are P_m, ρ_m, and u_m.

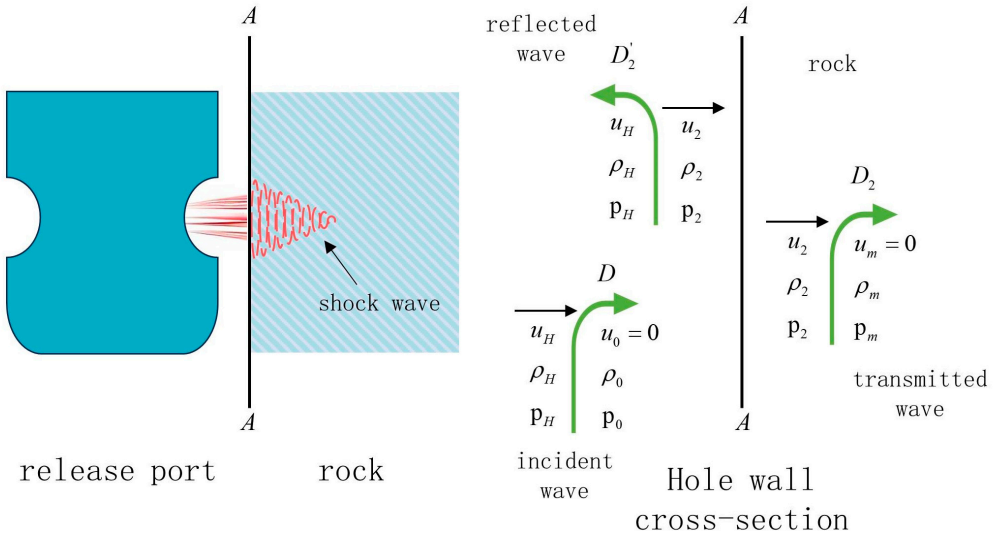


Figure 6. Schematic diagram of shock wave transmission and reflection.

According to the condition of stress continuity and displacement continuity at the stress wave interface, the incident wave, reflected wave, and transmitted wave satisfy the Snell theorem, and the expression for the incident rock stress at the borehole wall can be obtained as follows:

$$p_2 = p_H \frac{1+N}{1+N\rho_0 D/\rho_m D_2} \tag{14}$$

where p_2 is the hole wall incident rock stress, MPa; p_H is the supercritical CO_2 phase change impact pressure, MPa; N is the proportionality coefficient related to the nature of the medium, the metal, and rock media, the value of which is generally 1.1~1.2; $\rho_0 D$ is the impact impedance of CO_2; $\rho_m D_2$ is the impact impedance of the rock, expressed as Ω.

After the CO_2 phase change shock wave is incident on the rock body, it will spread to the far domain and gradually decay. The pressure decay equation is as follows [26]:

$$\sigma_r = p_2 \bar{r}^{-\alpha} \tag{15}$$

where $\bar{r}$ is the ratio distance, $\bar{r} = \mathrm{r}/r_b$; r is the line distance between the calculation point and the center of the borehole, m; r_b is the radius of the borehole, m; σ_r is the peak radial stress, MPa; α is the compressive stress attenuation index. For the shock wave, $\alpha \approx 3$.

Combining Equations (12)–(15) then yields a computational model for the attenuation of supercritical CO_2 phase change blasting shock waves in a rock medium, i.e.,

$$\sigma_r = \frac{2\sigma_s \delta \bar{r}^{-\alpha}(1+N)}{R\Omega + RN\left[\frac{2\sigma_s\delta(\mathrm{k}+1)}{RV_0}\right]^{1/2}} \tag{16}$$

Assuming that the fracturing tubes are all made of Q235 steel and the radii of the release holes are all 11 mm, and substituting the relevant coefficients, such as N and k, the radial stress at the hole wall is calculated as follows:

$$\sigma_r = \frac{693\delta}{0.011\Omega + 3.1715\sqrt{\delta\rho_0}} \tag{17}$$

It can be seen that the attenuation of supercritical CO_2 phase change blasting shock wave in rock medium is mainly related to the type of fracturing tube, the thickness of the shear sheet, and the shock impedance of the rock, in addition to the distance.

3.2. Decay Law of Supercritical CO_2 Phase Transition Shock Wave in the Rock Medium

As mentioned before, the CO_2 phase change shock pressure is mainly controlled by the thickness of the shear sheet, the shock wave velocity is controlled by the thickness of the shear sheet and the type of fracturing tube, and the shock impedance of the rock is controlled by the rock type. Therefore, to analyze the attenuation law of the shock wave under different factors, the relationship between each parameter and the incident rock stress at the borehole wall was analyzed based on the supercritical CO_2 phase change shock test by controlling the three variables of fracturing tube type, shear sheet thickness, and rock type, respectively. The specific analyzed working conditions are shown in Table 2.

Table 2. Shock wave attenuation influencing factors used to analyze working conditions.

Condition No.	Fracturing Tube Types	Shear Thickness/mm	Rock Type
1	51	3.4	granite
2	85	3.4	granite
3	100	3.4	granite
4	85	1.9	marble
5	85	2.6	marble
6	85	3.4	marble
7	100	2.6	shale
8	100	2.6	marble
9	100	2.6	granite

The values of the characteristic parameters of the fracturing tube are shown in Table 3, and the elastic properties of the rock are shown in Table 4.

Table 3. Characterization of different fracturing tubes.

Type	Outer Diameter/mm	Volume/m^3	CO_2 Filled Mass/kg	Initial Density/kg·m^{-3}
Type 51	51	5.8×10^{-4}	0.9	1.55×10^3
Type 85	83	1.57×10^{-3}	1.4	8.92×10^2
Type 100	95	4.21×10^{-3}	3.5	8.31×10^2

Table 4. Elastic properties of different rocks [27].

Rock Name	Density/kg·m^{-3}	Rock Wave Impedance/MPa
Shale	2.0	0.68
Marble	2.7	1.21
Granite	2.67	1.35

Combining Equations (12) and (13) and substituting all the above parameters into Equation (17), the peak radial stresses at the hole wall corresponding to each operating condition are obtained, as shown in Table 5.

Table 5. Calculation results of the peak radial stress for each working condition.

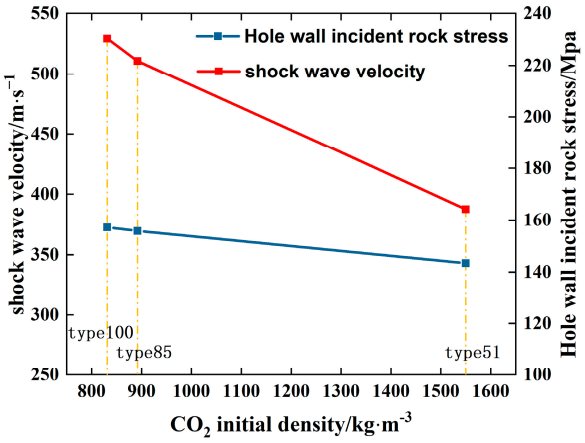
Serial Number	CO_2 Initial Density/k·m^{-3}	CO_2 Impact Pressure/MPa	Rock Wave Impedance/MPa	Shock Wave Velocity/m·s^{-1}	Incident Stress/MPa	Expansion Factor
1	1.55×10^3	101.69	1.35	387.61	143.37	1.41
2	8.92×10^2	101.69	1.35	510.95	155.72	1.53
3	8.31×10^2	101.69	1.35	529.37	157.20	1.55
4	8.92×10^2	56.83	1.21	381.97	91.12	1.60
5	8.92×10^2	77.76	1.21	446.80	119.87	1.54
6	8.92×10^2	101.69	1.21	510.95	150.99	1.48
7	8.31×10^2	77.76	0.68	462.91	100.66	1.29
8	8.31×10^2	77.76	1.21	462.91	120.99	1.56
9	8.31×10^2	77.76	1.35	462.91	124.33	1.60

Table 5 shows that compared with the CO_2 shock pressure, there is an obvious expansion effect of the hole wall incident stress, and the expansion coefficient is between 1.29 and 1.60. Combined with the calculated data in Tables 2 and 5, parameters such as fracturing tube type, shear sheet thickness, and rock type were controlled, while remaining unchanged, to analyze the changing rules of CO_2 phase change shock wave velocity and hole wall incident rock stress under the influence of different parameters, as shown in Figure 7.

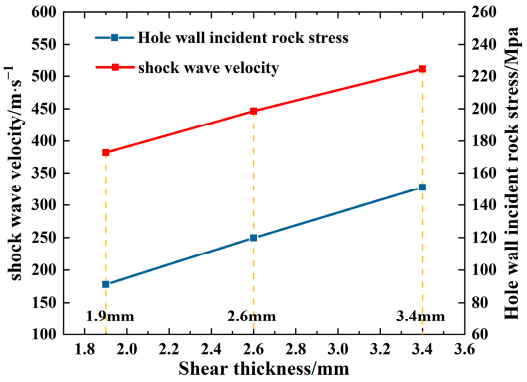
Figure 7 shows the effect curves of different initial densities of CO_2 in the fracturing tube, the thickness of the shear sheet, and rock wave impedance on the shock wave velocity and the incident stress on the borehole wall under the condition that the rest of the variables are constant. From Figure 7b, it can be seen that the increase in shear sheet thickness increases the shock wave velocity and the incident rock stress of the borehole wall linearly; Figure 7c shows that the rock wave impedance has no effect on the shock wave velocity, but it is positively correlated with the incident rock stress of the borehole wall.

To further explore the attenuation law of the shock wave in the rock medium, the specific distance parameter is added to analyze the propagation distance of the shock wave in the rock medium under the influence of the above three variables. The radius of the borehole under the three variables is adopted as the outer diameter of the type 85 fracture tube, and the distance of shock wave propagation in the rock medium is calculated by applying Equation (10) to the process of radial stress decreasing from the peak to zero. The results of the calculation are shown in Figure 8.

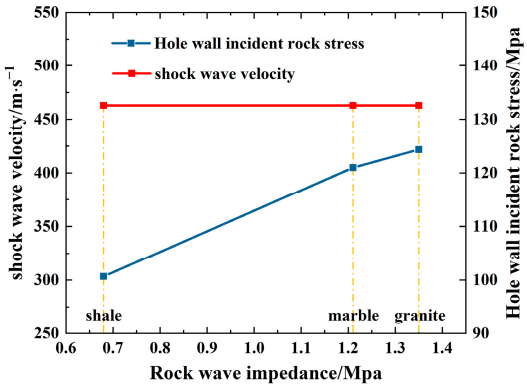
As shown in Figure 8, all the attenuation curves are logarithmically decaying, and the initial attenuation stresses are all the incident rock stresses at the borehole wall. As shown in Figure 8a, the propagation distances of shock waves corresponding to type 100, 85, and 51 fracturing tubes are 1.04 m, 1.04 m, and 1.01 m, respectively. It can be seen that with the CO_2-filled fracturing tubes, the fracturing tube type can affect the propagation distances of the supercritical CO_2 shock waves in the rock medium, and the propagation distances decrease with the increase in the filling density of CO_2. Similarly, Figure 8b,c also show that the shock wave propagation distance increases with the increase in shear sheet thickness and rock wave impedance.



(**a**) Variation curves of wave velocity and incident stress with different fracturing tubes.

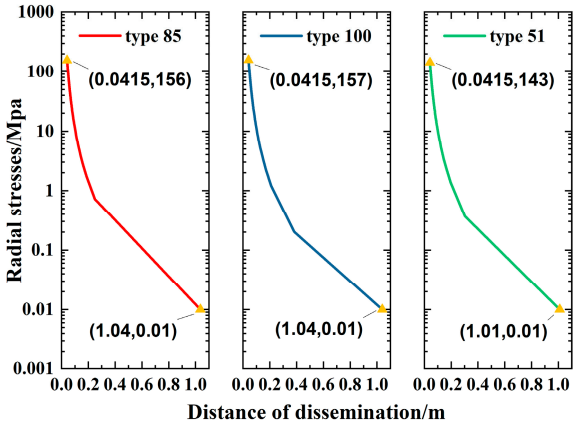


(**b**) Variation curves of wave velocity and incident stress under different shear sheets.

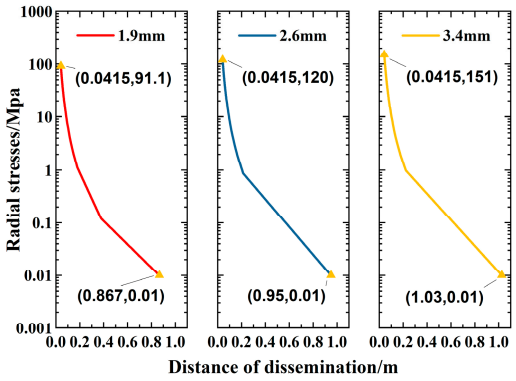


(**c**) Variation curves of wave velocity and incident stress for different rock types.

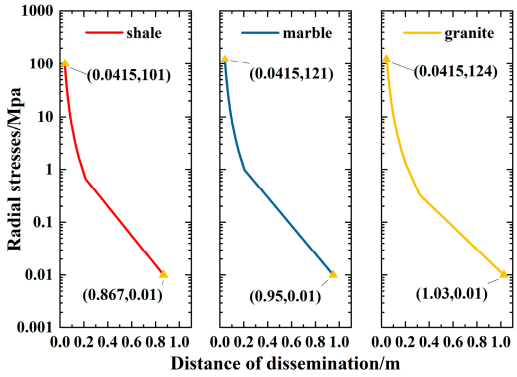
Figure 7. Variation curves of shock wave velocity and incident stress under the influence of different variables.



(**a**) Shock wave attenuation curves under different fracturing tubes.



(**b**) Shock wave attenuation curves under different shear sheets.



(**c**) Shock wave attenuation curves for different rock types.

Figure 8. Decay curves of supercritical CO_2 phase change blasting shock wave in rock medium.

4. Conclusions

In this paper, the generation process of the shock wave was analyzed according to the principle of supercritical CO_2 phase transition, and the propagation and attenuation law of shock waves was analyzed by considering CO_2 as an ideal gas. A supercritical CO_2 phase transition shock test was carried out, and a model for calculating the speed of the shock wave was established. The influencing factors of the incident rock stress at the borehole wall were analyzed, a propagation model of supercritical CO_2 phase transition shock wave in the rock medium was established, and the propagation distance under the influence of various factors was calculated. The supercritical CO_2 phase change shock wave propagation model in the rock medium was established, and the propagation distance under the influence of various factors was calculated.

(1) Based on the C–J theory, the calculation model of CO_2 phase transition shock pressure and other state parameters was established, and it was found that the supercritical CO_2 phase transition shock wave pressure is closely related to the shock wave velocity. The supercritical CO_2 phase transition shock test was carried out to analyze the shock pressure, and it was found that the shear damage formula can fit the test data very well, and the errors are all within 10%.

(2) Through Snell's theorem, an expression for the stress in the incident rock after the shock wave impact on the hole wall is given. The effects of type 100, 85, and 51 fracturing tubes, the thicknesses of 1.9 mm, 2.6 mm, and 3.4 mm shear sheets, and the performance parameters of three types of rocks, namely, shale, marble, and granite, on the incident rock stress on the borehole wall were further analyzed. It was found that the incident rock stress decreases with the increase in the initial density of CO_2 in the fracturing tube, increases linearly with the thickness of the shear sheet, and is positively correlated with the rock wave impedance. Moreover, there is an obvious expansion effect of the incident stress in the borehole wall compared with the CO_2 impact pressure, with the expansion coefficients ranging from 1.29 to 1.60.

(3) Based on the change rule of incident rock stress at the borehole wall, the attenuation distance of the shock wave in the rock medium under the influence of three variables was calculated separately, and the rock stress attenuation equation was established under the action of the phase change shock wave. It was found that the radial stress of the rock attenuates with the distance in a logarithmic manner, and with the increase in the distance, the propagation distance of the shock wave in the rock medium decreases with the elevation in the density of the filling of the CO_2, and it increases with the thickness of the shear sheet and the increase in the wave impedance in the rock.

Author Contributions: Conceptualization, J.Z., Q.Z. and L.L.; Methodology, F.W. (Fangqiang Wei), J.Z. and Q.Z.; Software, J.Z., F.W. (Fangqiang Wei) and Q.Z.; Formal analysis, J.Z., F.W. (Fangqiang Wei), L.L., Q.Z. and F.W. (Fayou Wu); Resources, J.Z. and L.L.; Data curation, Q.Z.; Writing—original draft, J.Z., Q.Z. and F.W. (Fangqiang Wei); Writing—review and editing, J.Z., Q.Z. and F.W. (Fangqiang Wei); Visualization, F.W. (Fangqiang Wei), L.L. and F.W. (Fayou Wu); Project administration, J.Z. and Q.Z.; Funding acquis, J.Z., Q.Z. and H.L. All authors have read and agreed to the published version of the manuscript.

Funding: This work was funded by the Chongqing Natural Science Foundation (CSTB2023NSCQ-MSX0913), the High-Level Talent Cultivation Program for Postgraduates of Tibet University (2021-GSP-S142), and the Chongqing Graduate Research Innovation Project (CYB23253, 2022S0023).

Data Availability Statement: No instructional records have been created or are compatible with the ongoing assessment data in this original copy.

Conflicts of Interest: The authors declare no conflict of interest.

References

1. Zhang, Y.; Deng, J.; Deng, H.; Ke, B. Peridynamics simulation of rock fracturing under liquid carbon dioxide blasting. *Int. J. Damage Mech.* **2018**, *28*, 1038–1052. [CrossRef]
2. Chen, H.D.; Wang, Z.F.; Qi, L.L.; An, F.H. Effect of liquid carbon dioxide phase change fracturing technology on gas drainage. *Arab. J. Geosci.* **2017**, *10*, 314. [CrossRef]
3. Gao, F.; Tang, L.; Zhou, K.; Zhang, Y.; Ke, B. Mechanism Analysis of Liquid Carbon Dioxide Phase Transition for Fracturing Rock Masses. *Energies* **2018**, *11*, 2909. [CrossRef]
4. Cheng, X.; Zhang, Z.; He, S.; Zhu, L. Research Status and Prospects of Liquid Carbon Dioxide Phase Transition Blasting Technology. *Coal Mine Blasting* **2022**, *40*, 10–15.
5. Liu, G.; Wang, H. Application Research on Carbon Dioxide Fracturing Technology. *Highway* **2018**, *63*, 72–75.
6. Lu, T.; Wang, Z.; Yang, H.; Yuan, P.; Han, Y.; Sun, X. Improvement of coal seam gas drainage by under-panel cross-strata stimulation using highly pressurized gas. *Int. J. Rock Mech. Min. Sci.* **2015**, *77*, 300–312. [CrossRef]
7. Xia, J.; Tao, L.; Li, B.; Zhou, M. Carbon dioxide liquid-gas phase change expansion rock breaking technology and application. *Eng. Blasting* **2018**, *24*, 50–54.
8. Guo, Z. Liquid Carbon Dioxide Blasting Cartridges and Field Test Blasts. *Blasting* **1994**, *3*, 72–74.
9. Xu, Y. Development of high pressure gas blasting coal mining technology and its application in China. *Blasting* **1998**, *1*, 67–69, 82.

10. Xue, F.; Xia, C.; Li, G.; Jin, B.; He, Y.; Fu, Y. Safety Threshold Determination for Blasting Vibration of the Lining in Existing Tunnels under Adjacent Tunnel Blasting. *Adv. Civ. Eng.* **2019**, *2019*, 8303420. [CrossRef]
11. Lv, G.; Zhou, C. Characteristics of Blasting Dynamic Damage of Tunnel Fault Zone Grouting Reinforced Perimeter Rock Body. *Chin. J. Rock Mech. Eng.* **2021**, *40*, 2038–2047.
12. Wang, X.; Hu, S.; Wang, E. Supercritical CO_2 Thermal Shock Rock Breaking Technology: Fracturing Principles and Vibration Safety Study. *China Civ. Eng. J.* **2023**, *56*, 118–130.
13. Gao, B.; Yang, Y.J.; Xue, W.L.; Guo, A.H.; Luo, X.D. Experimental Investigation on Influencing Factors of Rock Fragmentation Induced by Carbon Dioxide Phase Transition Fracturing. *Shock. Vib.* **2021**, *2021*, 6674485. [CrossRef]
14. Xia, J.; Dou, B.; Tian, H.; Zheng, J.; Cui, G.; Kashif, M. Research on Initiation of Carbon Dioxide Fracturing Pipe Using the Liquid Carbon Dioxide Phase-Transition Blasting Technology. *Energies* **2021**, *14*, 521. [CrossRef]
15. He, Z.; Zhang, S.; Jiang, N.; Luo, X.; Lei, Y. Experimental Study of CO_2 Phase Change Cracking Stress Wave Propagation and Influence Law. *Blasting* **2022**, *39*, 133–138.
16. Sun, K.; Wang, J.; Yu, X.; Li, W. Different Stress Difference Conditions of Supercritical CO_2 Gas Explosion Coal Rock Body Gas Wedge: Research on the Expansion Rule of Secondary Cracks. *Chin. J. Appl. Mech.* **2019**, *36*, 466–472, 516.
17. Guo, Y. Analysis of Liquid Carbon Dioxide Phase Change Fracturing Mechanism and Application Effect. Master's Thesis, Henan University of Science and Technology, Henan, China, 2017.
18. Ruan, R.; Pan, Z.; Wang, X.; Zhan, W. Study on ground vibration characteristics induced by liquid CO_2 blasting technique in bench excavation. *J. Vibroeng.* **2022**, *24*, 904–920. [CrossRef]
19. Li, B.; Wang, E.; Hu, S.; Wang, X.; Liu, B. A Study of Vibration Velocity Attenuation Induced by Pneumatic Rock Breaking with Carbon Dioxide Ice Powder for Safety Assessment. *Rock Mech. Rock Eng.* **2021**, *54*, 6481–6493. [CrossRef]
20. Zhou, S.; Jiang, N.; He, X.; Luo, X.D. Rock Breaking and Dynamic Response Characteristics of Carbon Dioxide Phase Transition Fracturing Considering the Gathering Energy Effect. *Energies* **2020**, *13*, 1336. [CrossRef]
21. Cheng, S. Protection of Adjacent Natural Gas Pipelines during Liquid CO_2 Phase Change Rock Breakups. *Eng. Blasting* **2023**, *29*, 69–77.
22. Li, Q.; Luo, D.; Feng, G. Dynamic Characteristics of Liquid CO_2 Phase Change Fracturing Using Experimental Technique. *Geotech. Geol. Eng.* **2019**, *37*, 3387–3398. [CrossRef]
23. Dai, J. *Dynamic Behaviors and Blasting Theory of Rock*; Metallurgical Industry Press: Beijing, China, 2014; pp. 121–132.
24. Abi, E.; Liu, L.; Pu, Y. A Protective Device for Filling with Supercritical Carbon Dioxide. Chinese Invention Patent P202211460376.1, 10 March 2023.
25. Abi, E.; Liu, L.; Pu, Y. A Supercritical Carbon Dioxide Tank Buffering Device. Invention Patent P202211526290.4, 28 March 2023.
26. Chu, H.; Yang, X.; Hou, A.; Yu, Y.; Liang, W. Experimental Study on Simulation of Propagation and Attenuation Law of Explosive Stress Wave in Coal Body. *Explos. Shock. Waves* **2012**, *32*, 185–189.
27. Wang, W. *Drill Hole and Blast*; Coal Industry Press: Beijing, China, 1984; pp. 1–13.

Disclaimer/Publisher's Note: The statements, opinions and data contained in all publications are solely those of the individual author(s) and contributor(s) and not of MDPI and/or the editor(s). MDPI and/or the editor(s) disclaim responsibility for any injury to people or property resulting from any ideas, methods, instructions or products referred to in the content.